J. Fluid Mech. (1990), *vol.* 214, *pp.* 1–15
Printed in Great Britain

Laboratory experiments on the cloud-top entrainment instability

By SHENQYANG S. SHY AND ROBERT E. BREIDENTHAL
Aeronautics and Astronautics, University of Washington, Seattle, WA 98195, USA

(Received 22 March 1989)

The stability of stratocumulus clouds with strong evaporative cooling effects is explored in laboratory simulations. Two fluids, initially separated by a thin horizontal plate, contain mixtures of water, alcohol and glycol which have a strongly nonlinear density as a function of mixture ratio. Initially, the fluid below the plate is more dense than that above the plate. When the plate is suddenly withdrawn, the turbulence in its wake mixes the two fluids together, producing mixtures with densities greater than that of either initial fluid. It is found that the system is unstable to strong perturbations only in cases of relatively large buoyancy reversal. The system is stable to strong perturbations if the buoyancy reversal is comparable to or less than the initial stratification. A simple model is presented to explain the results.

1. Introduction

The existence and persistence of stratus clouds play a significant role in the overall energy budget of the earth. Furthermore, real clouds are complex. Several processes may occur simultaneously, such as buoyancy increase due to evaporative cooling and radiative cooling. The latter has been simulated in the laboratory by McEwan & Paltridge (1976). The present work considers another facet of the overall atmospheric problem, simulated evaporative cooling.

Lilly (1968), Randall (1980) and Deardorff (1980) recognized that layer clouds may become unstable due to evaporative cooling and therefore may break up quickly if the air above them is not saturated. Randall suggested that instability would occur as long as the mixed parcels were even slightly negatively buoyant with respect to the underlying cloud. The reasoning was that the parcel would add turbulent kinetic energy to the flow and therefore increase the entrainment rate in a runaway manner. Contrary to the expectations of Randall and Deardorff, Turner & Yang (1963) found in their pioneer laboratory simulation of entrainment at the top of stratocumulus clouds that the entrainment rate was slightly reduced by this buoyancy reversal. However, in their experiments the Reynolds number based on the characteristic eddy lengthscale at the interface is estimated to be about 30. This may be below the liquid mixing transition (Weddell 1941; Breidenthal 1981) so that their results might not correspond to the fully turbulent flow.

It is important to make the distinction between a merely enhanced entrainment rate and instability. While evaporative cooling may increase the turbulent kinetic energy of the air below the inversion, if the stratification is still strong compared to the turbulence (large Richardson number), the entrainment rate may still be quite modest. For example, in Randall's view, evaporative cooling would play no direct dynamic role at the interface except to agitate the air below the cloudtop. This is

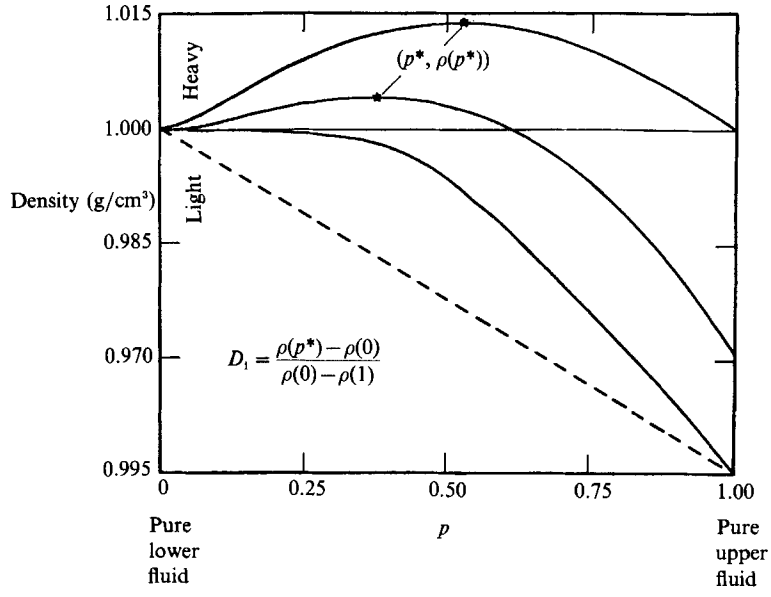

FIGURE 1. Mixing density as a function of mixture fraction p of upper fluid. The solid lines represent the nonlinear case, consisting of alcohol and glycol mixtures in various proportions, mixing with water, one with a mixture of 40.4% alcohol and 59.6% glycol ($D_1 \approx \infty$), one with a mixture of 50.5% alcohol and 49.5% glycol ($D_1 = 0.14$) and one with a mixture of about 55% alcohol and 45% glycol ($D_1 = 0$), using the same fluid system as Turner (1966). The dashed line represents the linear case (environment saturated).

contrasted with the issue of instability, by which we mean whether or not a disturbance would grow in time so that the cloud would break up relatively rapidly even if the source of the initial perturbation is removed.

This note addresses the following questions: What are the conditions for instability? What precisely is meant by instability? What is the physical mechanism that determines instability? The impact of buoyancy reversal as well as the effect of Richardson number on the entrainment rate and instability under different forcing for what we shall call the stirred-grid experiment are not discussed here, but will be reported in the near future.

2. Experimental methods

2.1. *Density as a function of mixture ratio*

The evaporative cooling in atmospheric clouds produces mixtures whose density can be greater than either parent parcel. In clouds, the density relationship is composed of two essentially straight lines. In the laboratory, an imperfect approximation to this has been realized. Density is plotted as a function of the mixture fraction of the upper fluid for water–alcohol mixtures in figure 1, using the same fluid system as Turner (1966). Glycol is added to the alcohol in order to raise the density nearer to that of water. The density is a maximum at a mixture fraction $p = p^*$. For these experiments, p^* is in the range of about 0.3–0.7. The range can be extended from 0.1 to 0.7 by adding appropriate amounts of potassium iodide and glycerine into the two fluids.

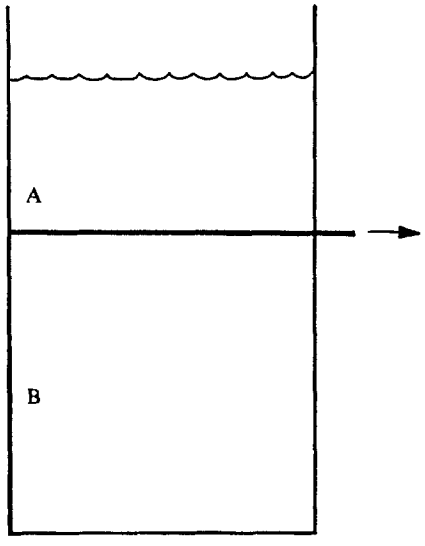

FIGURE 2. Sketch of the apparatus. A, mixtures of alcohol and glycol. B, water.

A dimensionless buoyancy reversal parameter is defined as follows;

$$D \equiv \frac{\rho(p^*)-\rho(p)}{\rho(p)-\rho(1)} \quad \text{for} \quad p < p^*. \tag{1}$$

It indicates the ratio of the maximum density change at p^* to the density difference between the two layers of fluid. $\rho(p)$ is the density of mixed fluid consisting of p parts of the pure upper fluid and $(1-p)$ parts of the pure lower fluid; $\rho(1)$ is the density of the pure upper fluid (the simulated dry, unsaturated layer). $\rho(0)$ is the density of the pure lower fluid (the simulated cloud). Before a run, the initial value of D, D_i, was selected from a value between 0 and 15 for these experiments.

2.2. *The apparatus*

The apparatus is sketched in figure 2. Two lucite mixing boxes with different geometries were used, a vertical circular cylinder of 15 cm inside diameter and 30 cm height which we call the 'small box' and one 28 cm × 28 cm × 60 cm height, the 'large box'. Both boxes were separated into two compartments by a thin, horizontal sliding stainless steel plate of 0.07 cm thickness. Before a run, the compartment below the plate was filled with water and that above the plate with a mixture of alcohol and glycol.

2.3. *Flow visualization technique*

Using phenolphthalein, a pH indicator, in one fluid and sodium hydroxide in the other fluid, the initially colourless fluids became dark red upon mixing. The volume mixing ratio of lower to upper fluid at which this occurs is the equivalence ratio ϕ. For these experiments, ϕ was chosen to be about 20. That is to say that 100 cm^3 of the lower fluid only needs 5 cm^3 of the upper fluid to turn the colour on. The chemistry is fast, so the Dämkohler number is effectively infinite. A run began with initially quiescent fluids. The dividing plate was quickly withdrawn, leaving a turbulent wake as a strong perturbation at the interface. The subsequent behaviour of the system was recorded on film and video tape.

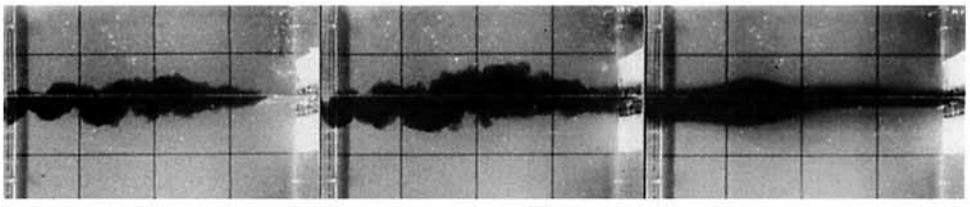

(a) (b) (c)

FIGURE 3. The evolution of the linear experiment at three different times. (a) 0.98 s; (b) 2.5 s; (c) 45.4 s.

3. Results

It is important that the initial perturbation be sufficiently large at the interface to ensure that the flow is above the mixing transition, a consequence of the appearance and development of small-scale three-dimensional motions in the flow (Weddell 1941; Konard 1977; Breidenthal 1981; Broadwell & Breidenthal 1982), so that the results correspond to the high-Reynolds-number atmospheric case. The plate was rapidly withdrawn to create a fully turbulent wake at the interface, where the Richardson number based on the thickness of the wake, its maximum density difference with underlying fluid, and the average speed of the withdrawing plate was small ($Ri < 1$). Then the behaviour of the interface depended on the initial $D = D_i$.

3.1. *Flow structure*

The results of several runs are described. The initial value of the buoyancy reversal parameter is D_i.

3.1.1. *Linear case*, $D_i = 0$

The initial disturbance decayed quickly. The mixture was intermediate in density, between that of the two initial fluids, and therefore it accumulated at the inversion. The evolution of the experiment at different stages is shown in figure 3.

3.1.2. *Nonlinear case*, $D_i > 0$

(a) $D_i = 0.2$

Figure 4 shows the evolution of the system at different times for relatively weak nonlinearity. After the plate was withdrawn, the heavy mixed parcel descended as a downward movement of thermal convection. It slowly detached itself from the interface without significant additional engulfment from above. Note that the interface remained almost flat. Eventually the system became quiescent. At 40 s for the small box and 100 s for the large box, samples of the fluid at the bottom of each tank and just below the interface were taken to determine their composition and the current value of D. The surviving upper-layer fluid remained pure and colourless. We also measured its thickness to determine how much dilution occurred of the lower fluid layer (the simulated cloud) by the upper fluid layer (the simulated dry air) from such a turbulent event. These measurements were repeated at 5 and 10 min. Neither the composition of the bottom fluid nor D changed significantly during this time.

(b) $D_i = 1.0$

Figure 5 shows the evolution of the flow at four times. The results are qualitatively similar to that for $D_i = 0.2$. The interface tilted gently and then promptly returned

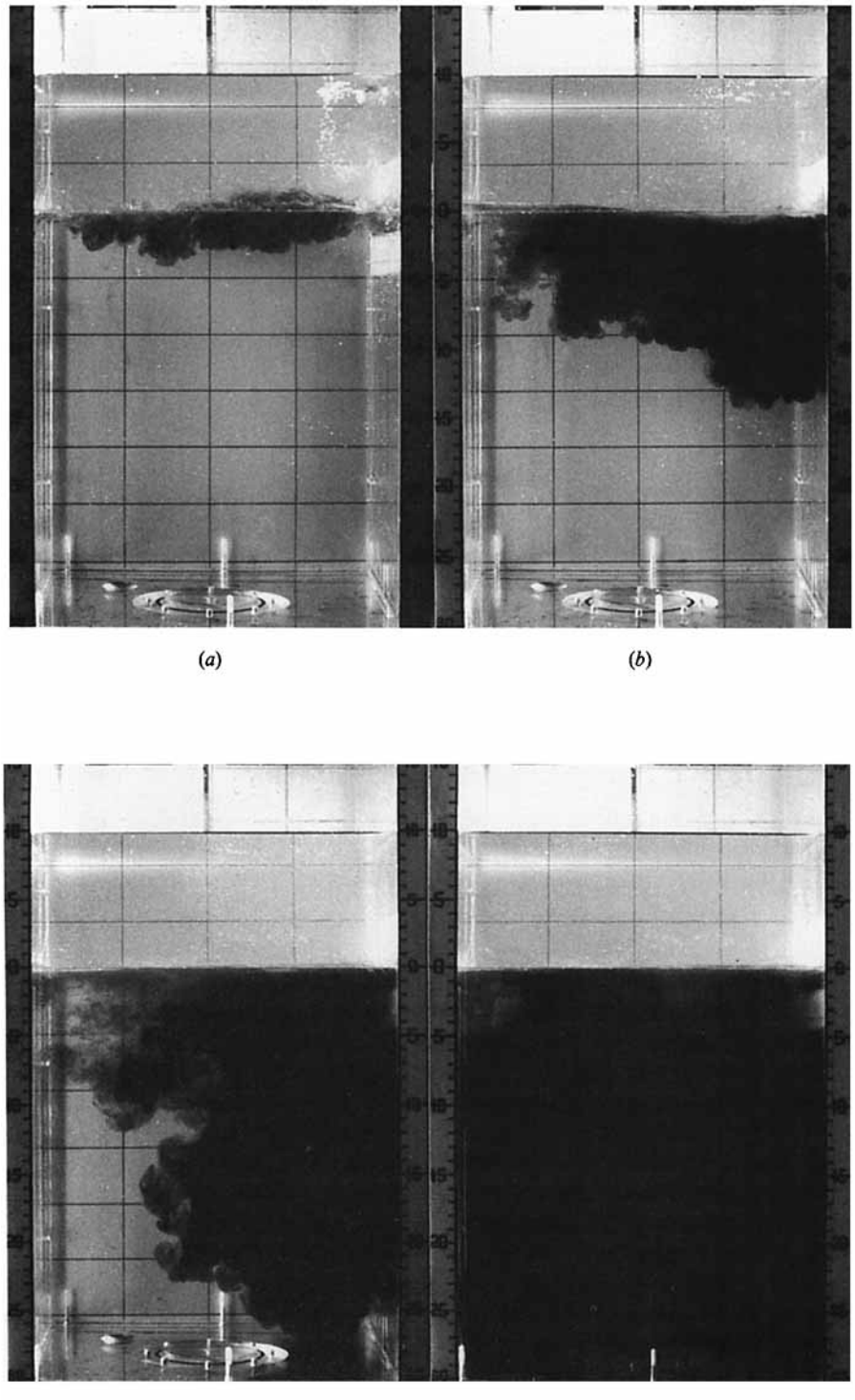

FIGURE 4. The evolution of the system for $D_i = 0.2$. (*a*) 0.94 s; (*b*) 5.7 s; (*c*) 13.8 s; (*d*) 44.7 s.

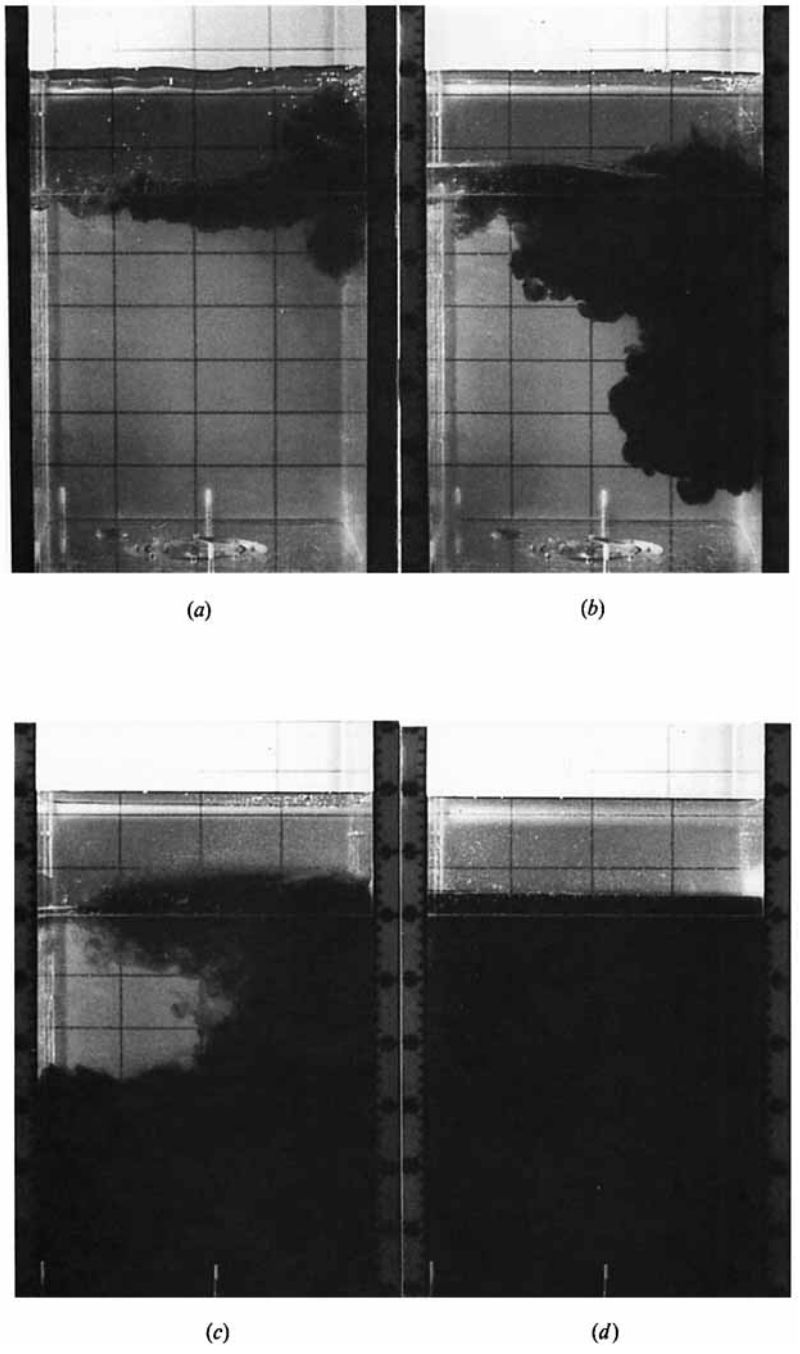

FIGURE 5. The evolution of the flow for $D_i = 1.0$. (*a*) 1.2 s; (*b*) 7.2 s; (*c*) 13.4 s; (*d*) 46.8 s.

back to horizontal after the heavy mixed parcel descended. Compared to the case of $D_i = 0.2$, there was more dilution of the lower fluid by the upper fluid as indicated by the final rise of the stratified interface. After the turbulence decayed, the only remaining motion was associated with laminar dripping of mixed fluid from many convective cells at the interface.

(*c*) $D_i = 2.0$

Figure 6 shows the evolution of the flow at four different times for a case of stronger buoyancy reversal. Again the heavy, mixed fluid produced by the initial perturbation descended. However, a distinct difference was observed in the interface for this case. It became strongly tilted. The flow was unstable in the sense that the perturbed interface did not relax back to horizontal, but developed a strong tilt. Evidently, the heavy, descending fluid formed a vortex structure which tilted the interface, which in turn fed the structure fresh fluid from above, thereby maintaining the heavy structure as it grew and descended. Soon, however, the walls constrained the flow as the structure filled the lower region and consumed all the lower fluid. Then the effective value of D across the inversion was reduced, and the Richardson number was increased. The system became stable again. Fluid samples extracted from the boxes during all runs where D_i was greater than 1.0 indicated that the final value of D had been reduced to the range 0.7–1.3. From the height of the surviving upper fluid, it is clear that much more entrainment had occurred in these cases than those where $D_i \leqslant 1.0$ under the same initial perturbation.

(*d*) $D_i = 5.0$

Figure 7 shows the evolution of the flows at four different times for $D_i = 5.0$. The results are qualitatively similar to that for $D_i = 2.0$. The interface tilt is even more pronounced. It is unstable in the sense that an entrained tongue of pure upper fluid would dip down because of strong buoyancy reversal, leading to a plume-like runaway entrainment. Sustained vigorous entrainment occurred until the walls limited growth.

3.2. *Instability condition*

3.2.1. *Evolution of D with time*

In figure 8 the buoyancy reversal parameter D is plotted as a function of time for many runs with widely varying initial values of D for the small mixing box. The straight lines connect the corresponding points from each run over the time interval when no measurements of D were made. The results for the large box are qualitatively the same as those for the small box, except for a time lag. Figure 9 shows D at 40 s in the small box and at 100 s in the large box as a function of its initial value. We saw above that for D_i greater than 1.3, under strong perturbation, the interface became strongly tilted to form a tongue of upper fluid which descended below the level of the undisturbed inversion. This tongue was engulfed into the descending parcel. Runaway entrainment proceeded until a large enough fraction of upper fluid was mixed into the lower fluid to change the composition to where D was reduced to be about 1.

For $D_i \leqslant 1.0$, under the same initial perturbation, the heavy mixed parcel sank, but it did not trigger the additional entrainment of upper fluid. Consequently, D did not change significantly during a run.

3.2.2. *The role of the lower boundary*

A true interface instability should only depend on the conditions at the interface, not on the presence or proximity of a lower boundary (the bottom of the tank). We therefore used two different tanks with varying layer depths and widths to test for the sensitivity to the lower boundary. A layer-depth ratio (LDR) denotes the ratio of the lower-layer depth to the upper-layer depth before a run. We set LDR = 2 for

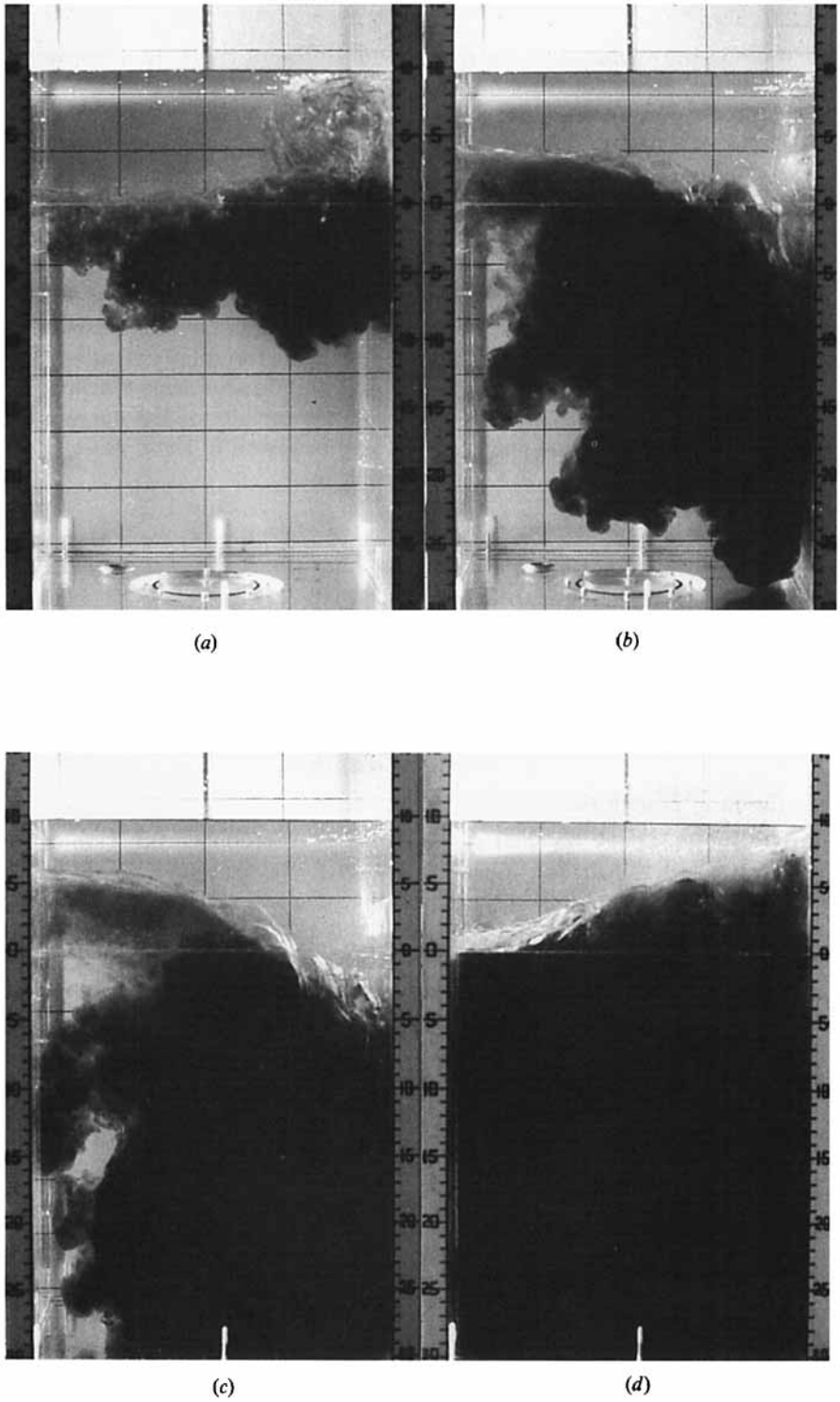

FIGURE 6. The evolution of the flow for $D_1 = 2.0$. (a) 3.7 s; (b) 7.4 s; (c) 9.9 s; (d) 27.4 s.

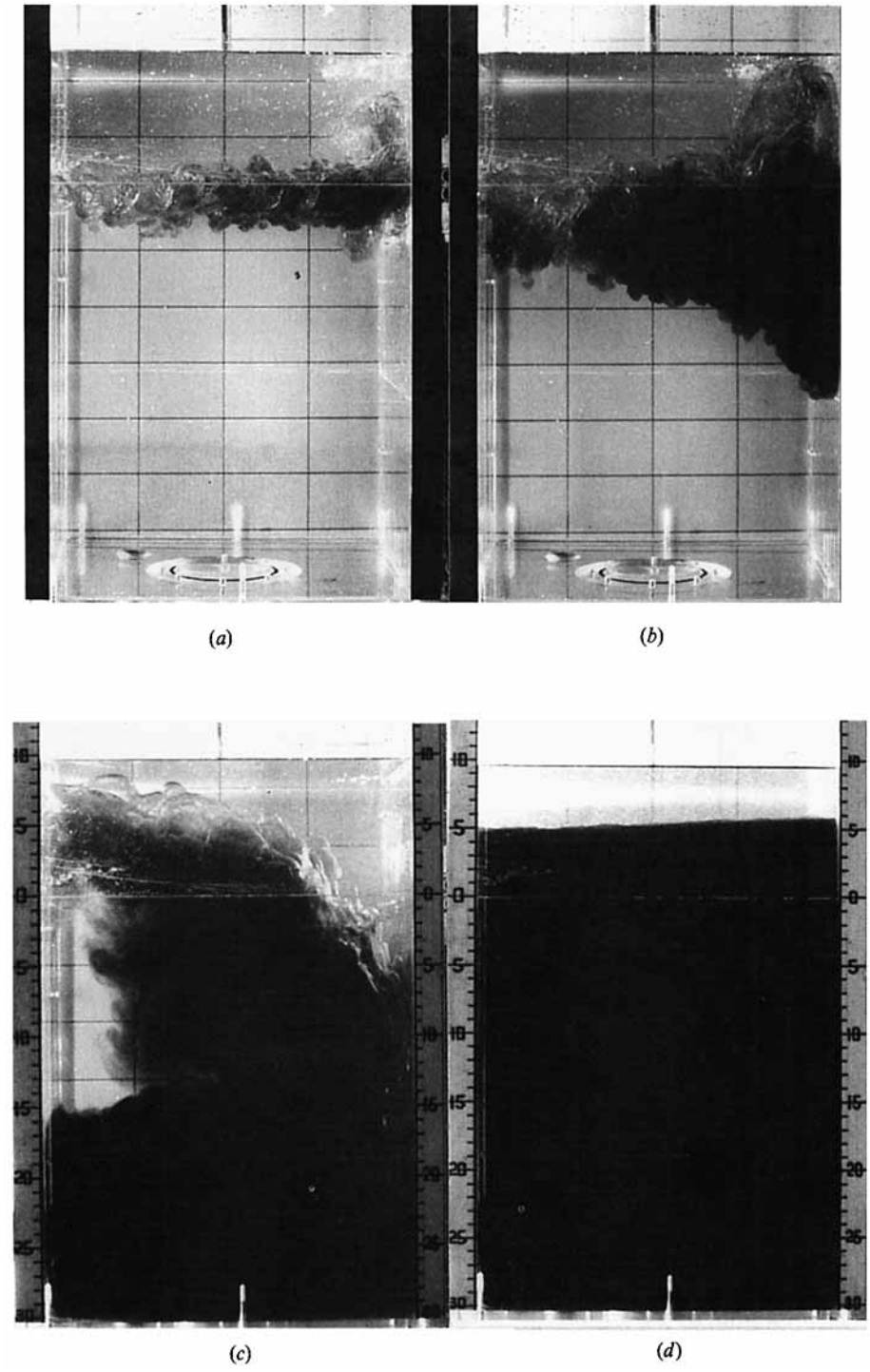

FIGURE 7. The evolution of the flow for $D_1 = 5.0$. (*a*) 1.0 s; (*b*) 3.5 s; (*c*) 9.9 s; (*d*) 97.2 s.

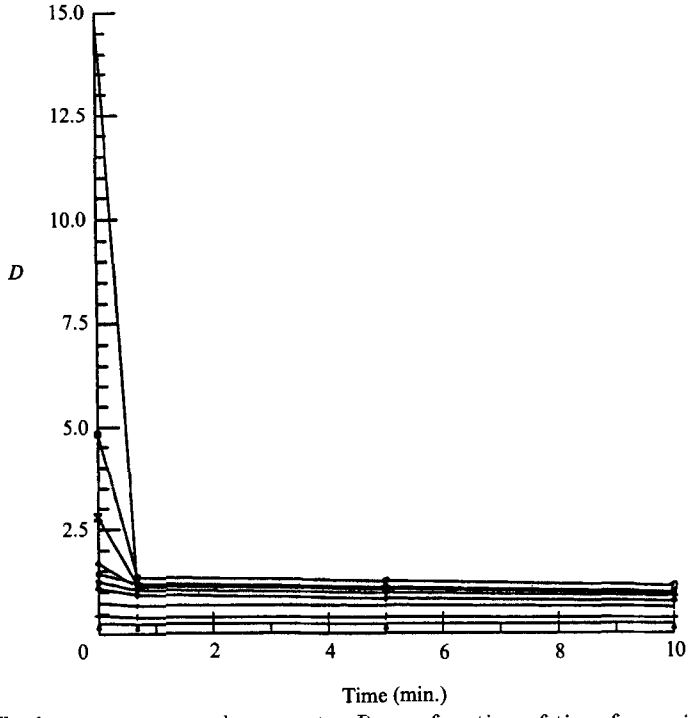

FIGURE 8. The buoyancy reversal parameter D as a function of time for various initial value D_i.

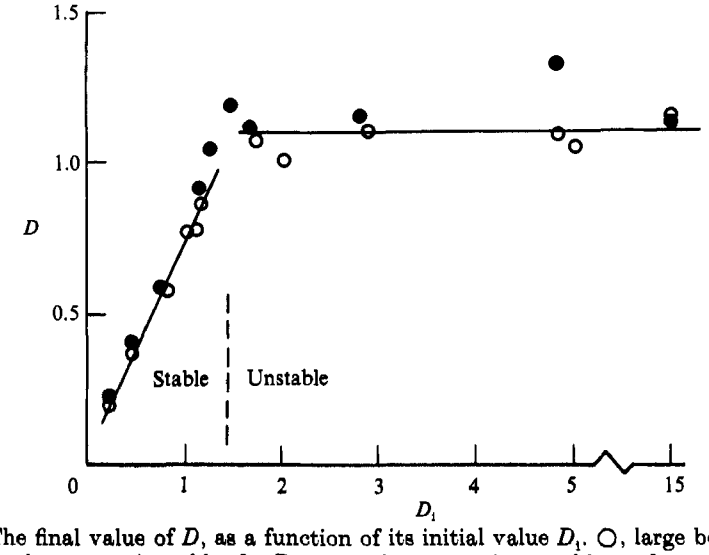

FIGURE 9. The final value of D, as a function of its initial value D_i. ○, large box; ●, small box. For $D_i < 1.0$, the system is stable; for $D_i > 1.3$, the system is unstable, under strong perturbation.

the small box and LDR = 3 for the large box. The results of the two mixing boxes are remarkably similar, as shown in figure 9. The critical value of D for instability was evidently not influenced by the lower boundary in these simple experiments.

3.2.3. *The role of the sidewalls*

For these experiments, the average thickness of turbulent wake at the interface, which was measured just after withdrawing the plate, was typically about 5 cm for

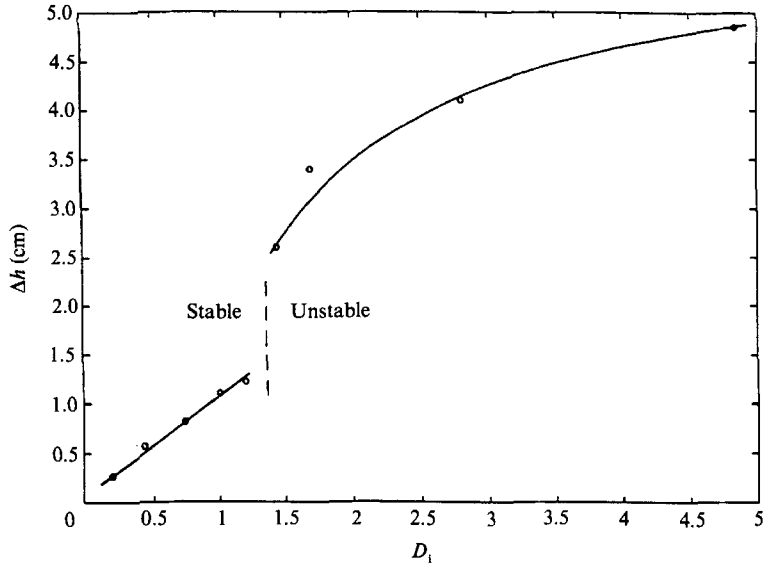

FIGURE 10. The entrained fluid as a function of buoyancy reversal parameter for large box experiments.

the small box and 7 cm for the large box under approximately the same withdrawing speed of the sliding plate. We then define a normalized width ratio (WD) which is the width of the boxes to the average thickness of the turbulent wake. For the small box, WD ≈ 3; for the large box, WD ≈ 4. Even though the wake following the withdrawn plate accumulates near one wall, it appears that the box width plays no role in the basic results as shown in figure 9. Experiments, not reported here, using an oscillating grid to generate the perturbations on a surface region everywhere instead of a turbulent wake indicate the same critical value for D_i. This is expected as long as the perturbation is of sufficiently small Richardson number and large Reynolds number based on the eddy size near the interface to create the fully turbulent mixing.

3.2.4. *The sensitivity of the initial perturbation*

Gradual withdrawal of the plate, causing only a small disturbance, is associated with a large Richardson number and small Reynolds number based on the thickness of the wake, such that the runaway entrainment did not occur for D_i as large as 10. The heavy mixtures generated by this small perturbation descended slowly and resulted in a laminar convective motion in the lower-layer fluid that slowly entrained the layer of fluid above. This process continued until D became zero, when the mixtures were no longer heavier than the lower fluid (saturated environment). Although this phenomenon is important in nature, the present experiments are designed to investigate the case where the perturbations are driven from the turbulent source instead.

3.3. *Entrainment in a tank of finite depth*

The total amount of entrained fluid during the course of a run was measured by observing the change in height Δh of the upper fluid diluted into the lower fluid from the initial state ($t = 0$) to a time when the interface was approximately flat (40 s for the small box and 100 s for the large box). The effect of the simulated evaporative cooling on entrained fluid is shown in figure 10. There is a linear increase of entrained

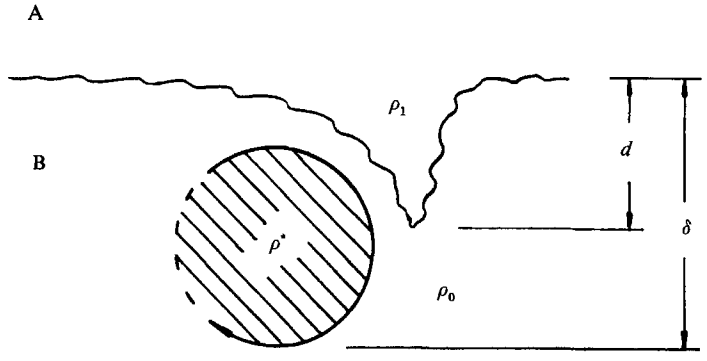

FIGURE 11. Model of the entrainment process and the instability.

fluid with D_i for $D_i < 1$, followed by a more rapid rise as D_i increases above the threshold value of 1.3. Results for the instantaneous entrainment rate $E \equiv w_e/w$, where $w_e \equiv \mathrm{d}z/\mathrm{d}t$ and w is local turbulent velocity scale near the interface, as a function of the buoyancy reversal parameter and Richardson number, using grid turbulence, will be presented in a forthcoming paper.

4. Discussion

The central surprise of these results is that the system is stable to strong perturbations unless the initial buoyancy reversal parameter D_i is greater than about 1.3. For $D_i \leqslant 1.0$, the mixing is largely confined to that of the initial strong perturbation without much additional engulfment of upper fluid. The heavy fluid sinks and the initial disturbance decays. For $D_i \geqslant 1.3$, however, the interface is tilted strongly owing to the large buoyancy reversal to form an entrained tongue of upper fluid. The growth of this rapidly entraining structure is sustained until it is inhibited by the size of the container. Then the effective value of D across the inversion is below the critical value of D and the turbulent motions eventually subside.

It is clear that the original view of the instability cannot explain these results. It predicted that the critical value of D is essentially zero, so that any heavy, mixed parcels produced would, upon falling, energize the turbulence in the lower fluid enough to precipitate enough additional mixing to generate runaway entrainment. Evidently, the mere production of heavy mixed fluid is not a sufficient condition for instability.

A key element is the feature of the entrainment tongue observed only for unstable cases. As in many other turbulent flows, entrainment is controlled by large-scale engulfment (Roshko 1976). In contrast to large-scale engulfment, small-scale nibbling is apparently negligible. It is reasonable to suppose that the two-layer system is unstable only if the heavy fluid can form, as it descends into the lower fluid, a tongue with which to feed itself more upper fluid, leading to a plume like runaway entrainment as shown in figures 6 and 7. Such a tongue is presumably required to supply the appetite and maintain the health of a growing, unstable vortex.

Here we present a simple physical model, a related version reported by Siems *et al.* (1990). Imagine a vortex of heavy mixture spinning as it descends into pure, lower fluid (figure 11). If it is in equilibrium, its effective rotation rate Ω of the vortex is

related to its diameter δ and its buoyancy difference with its environment g' by the requirement that its equilibrium Richardson number is approximately unity. Then

$$\Omega \approx \left(\frac{g'}{\delta}\right)^{\frac{1}{2}}, \tag{2}$$

where

$$g' \equiv \frac{\rho(p^*)-\rho(0)}{\rho(0)} g.$$

For simplicity, we have assumed that the vortex has the maximum possible density $\rho(p^*)$. This is reasonable because the vortex with $Ri \approx 1$ can directly engulf and mix the fluids by its motion.

Now consider the maximum depth such a vortex can draw down a tongue of light, upper fluid. This distance d is

$$d = \frac{V^2}{g''}, \tag{3}$$

where V is the maximum tangential velocity of the vortex and g'' is the buoyancy between pure upper and lower fluids.

$$g'' \equiv \frac{\rho(0)-\rho(1)}{\rho(0)} g. \tag{4}$$

Now $V \approx \Omega\delta$, so from (2) and (3),

$$d \approx \frac{g'}{g''}\delta.$$

Then

$$\frac{g'}{g''} = \frac{\rho(p^*)-\rho(0)}{\rho(0)-\rho(1)} \equiv D_{\mathrm{i}},$$

we have

$$\frac{d}{\delta} \approx D_{\mathrm{i}}. \tag{5}$$

The ratio of the maximum possible tongue size d to the vortex size δ is approximately D_{i}.

If D_{i} is less than unity, the vortex cannot pull down the tongue very far in terms of the vortex diameter ($d < \delta$) owing to its relatively weak buoyancy reversal. A complete rotation of the tongue around the vortex is not possible. Consequently, the vortex cannot incorporate the additional fresh upper fluid as it descends. Its influence on the interface then declines, and the tilted interface (tongue) will rebound back to horizontal because of its lighter density. But for some value of D_{i} of order unity, the vortex has great enough density to pull the tongue down further and wrap it around itself. It entrains the upper fluid, mixes it with the lower fluid, and maintains its density. With no intrinsic lengthscale in the problem, a self-similar solution is expected, with the vortex and tongue both growing. The ratio of their sizes is only a function of D_{i} if the initial disturbance is large enough to ensure that the flow is fully turbulent mixing. Growth proceeds at an accelerating rate until the walls limit it.

The transition from stable to unstable behaviour is sharp because the criterion for instability depends on the rotation of a buoyant tongue around a negatively buoyant vortex. Unless the tongue can be drawn down and around the vortex the amount of

mixing is modest. Indeed, other experimental results, to be reported in a forthcoming paper, indicate that the entrainment rate under continual forcing is a weak function of D below the instability transition.

5. Conclusion

A series of simple laboratory experiments reveal that a stratified interface is stable to buoyancy reversal from turbulent mixing until the magnitude of the reversal is comparable to the initial stratification. Associated with the instability is the occurrence of a tongue of upper fluid drawn down by the descending, mixed, heavy fluid. For instability, a simple model assumes that the tongue must extend to the level of a vortex of heavy, mixed fluid for sufficient mixing to occur. Then the descending vortex structure is invigorated with additional heavy, mixing fluid as it grows so as to maintain its supply of upper fluid through the tongue. This structure would be sustained until the confines of its enclosure preclude further growth.

The laboratory results may be related to the behaviour of marine stratocumulus clouds. These clouds' remarkable longevity in the face of finite D indicates that they can be stable (Hanson 1984; Albrecht, Penc & Schubert 1985; Siems *et al.* 1990). The present work suggests that buoyancy reversal as well as the perturbation must be large for instability. These results may also be related to the instability in the Weddell Sea off Antarctica (Cabbeling instability) where the density of salt water mixtures may be greater than that of the constituent parcels (Foster 1972; Foster & Carmack 1976).

The authors wish to thank Professor Marcia Baker for introducing the problem to us and for many stimulating discussions. We also benefited from interactions with Professor Chris Bretherton, Professor David Randall, and Mr Steve Siems. This research was supported by NSF Grant ATM-8611225A02.

REFERENCES

Albrecht, B. A., Penc, R. S. & Schubert, W. H. 1985 An observational study of cloud-topped mixed layers. *J. Atmos. Sci.* **42**, 800–821.

Breidenthal, R. E. 1981 Structure of turbulent mixing layers and wakes using a chemical reaction. *J. Fluid Mech.* **109**, 1–24.

Broadwell, J. E. & Breidenthal, R. E. 1982 A simple model of mixing and chemical reaction in a turbulent shear layer. *J. Fluid Mech.* **125**, 397–410.

Deardorff, J. W. 1980 Cloud-top entrainment instability. *J. Atmos. Sci.* **37**, 131–147.

Foster, T. D. 1972 An analysis of the cabbeling instability in sea water. *J. Phys. Oceanogr.* **2**, 294–301.

Foster, T. D. & Carmack, E. C. 1976 Temperature and salinity structure in the Weddell Sea. *J. Phys. Oceanogr.* **6**, 36–44.

Hanson, H. P. 1984 On mixed-layer modelling of the stratocumulus topped marine boundary layer. *J. Atmos. Sci.* **41**, 1226–1234.

Konrad, J. H. 1977 An experimental investigation of mixing in two-dimensional turbulent shear flows with application of diffusion-limited chemical reactions. PhD thesis, California Institute of Technology. Reprinted as Project SQUID Tech. Rep. CIT-8-PU, Dec. 1978.

Lilly, D. K. 1968 Models of cloud-topped mixed layers under a strong inversion. *Q. J. R. Met. Soc.* **94**, 292–309.

McEwan, A. D. & Paltridge, G. W. 1976 Radiatively driven thermal convection bounded by an inversion – A laboratory simulation of stratus clouds. *J. Geophys. Res.* **81**, 1095–1102.

RANDALL, D. S. 1980 Conditional instability of the first kind upside-down. *J. Atmos. Sci.* **37**, 125–130.

ROSHKO, A. 1976 Structure of turbulent shear flows: A new look. *AIAA J.* **14**, 1349–1357.

SIEMS, S. T., BRETHERTON, C. S., BAKER, M. B., SHY, S. S. & BREIDENTHAL, R. E. 1990 Buoyancy reversal and cloudtop entrainment instability. To appear in *Q. J. R. Met. Soc.*

TURNER, J. S. 1966 Jets and plumes with negative or reversing buoyancy. *J. Fluid Mech.* **26**, 779–792.

TURNER, J. S. & YANG, I. K. 1963 Turbulent mixing at the top of stratocumulus clouds. *J. Fluid Mech.* **17**, 212–224.

WEDDELL, D. 1941 Turbulent mixing in gas flames. PhD thesis, Massachusetts Institute of Technology, 115.